This article has been accepted for inclusion in a future issue of this journal. Content is final as presented, with the exception of pagination.

Analysis and Implementation of High-*Q* CT Inductor for Compact and Wide-Tuning Range *Ku*-Band VCO

Islam Mansour, Mohamed Aboualalaa, Adel Barakat, *Member, IEEE*, Ahmed Allam, Adel B. Abdel-Rahman, Mohammed Abo-Zahhad, and Ramesh K. Pokharel, *Member, IEEE*

***Abstract*—This work presents a new structure of center tap (CT) inductor to improve the performance of *Ku*-band voltage-controlled oscillators (VCOs). Conventional CT inductor provided by the foundry suffers from a poor-quality (*Q*-) factor large area and low self-resonance frequency. These problems are solved by introducing a coupling structure. For the proposed CT inductor, despite its size is miniaturized by 51%, the *Q*-factor is increased by 41% in the frequency range of 5–30 GHz compared to a conventional CT inductor. The measured differential inductance and quality factor of the proposed inductor are 385 pH and 22 at 12 GHz. The proposed CT inductor is used to design a compact and wide-tuning-range VCO at *Ku*-band in 0.18-μm complementary metal–oxide–semiconductor (CMOS) technology, and this leads to 5.8 dB phase noise improvement compared to the use of a conventional CT inductor. The fabricated VCO has a compact core size of 140 μm × 400 μm only. The VCO chip oscillates from 11.7 to 13.7 GHz. The measured phase noise is −107.7 dBc/Hz at 1-MHz offset frequency at a carrier frequency of 13.7 GHz, and the dc power consumption of the VCO core is 4 mW which results in a figure of merit (FoM) normalized to the die area ($\mathrm{FoM_A}$) to be −197 dBc/Hz.**

***Index Terms*—Center tap (CT) inductor, figure of merit (FoM), *Ku*-band voltage-controlled oscillator (VCO), phase noise, tuning range.**

I. Introduction

MINIATURIZATION of each building block of a complementary metal–oxide–semiconductor (CMOS) transceiver is important to reduce the overall cost of a system. Miniaturization is a challenge especially in radio frequency integrated circuits (RFIC) as it is, typically, associated with the degradation of quality (*Q*-) factor of the passive components and the resulting system signal-to-noise ratio [1], [2]. These passive components include the inductors and the transmission lines, which are major subcomponents of voltage-controlled oscillators (VCOs), amplifiers, matching circuits and mixers. In the case of a VCO, miniaturization usually worsens the VCO's performance in terms of the phase noise and the power consumption [3]–[7].

The VCOs at *X*-band [3] and *K*-band [4] employing stacked inductors [1] were very compact. However, these VCOs suffered from a poor phase noise of −93 dBc/Hz at 1-MHz offset frequency. In [8], a wide-tuning-range VCO using the switching capacitor was proposed. In most of the cases, the VCO exhibits poor phase noise at higher frequencies which limits their applications in wireless communication systems.

According to Leeson's phase-noise model [9], to improve the phase-noise characteristics, the *LC* oscillator tank must have a high *Q*-factor at the required oscillation frequency. Inductor quality factor improvement can be achieved by changing geometry and layout optimization [10]–[13]. For example, Yue and Wong [11] proposed using a patterned ground shield in the lower layers to isolate the inductor from the lossy substrate. Zou *et al.* [12] designed an eight-shaped inductor which consists of two twisted constitutive loops and a good differential quality factor of ∼15 at 10 GHz and ∼17 at 13 GHz was obtained. While in [13], variable width and spaced (tapered) spiral rectangular inductor are optimized to increase the *Q*-factor and achieves a peak-*Q* value of 16.6 at 7 GHz.

In this letter, first, a compact and high *Q*-factor center tap (CT) inductor is proposed. By exploiting the tight coupling between two arms of the CT inductor, the size is compacted. Furthermore, the self-inductance has wideband characteristics from 5 to 30 GHz, and additionally, the *Q*-factor is improved almost by 41% compared to a conventional CT inductor provided by the foundry. Then, a wide-tuning-range VCO using this CT inductor is designed and implemented in 0.18-μm CMOS technology. The measurement shows that the phase noise of the proposed VCO is comparable to the state-of-the-art VCOs [2], [5], [8] of the same carrier frequency that implemented in the similar CMOS technology, but chip size and tuning range are significantly improved.

II. Proposed CT Inductor

There are different shapes of spiral inductors as square, hexagonal, octagonal, and circular shapes. The inductance value is directly proportional to the length of the current path. Fig. 1(a) shows the layout of a conventional inductor and the

Manuscript received June 2, 2020; accepted June 22, 2020. *(Corresponding author: Islam Mansour.)*

Islam Mansour is with the Electrical Engineering Department, Shoubra Faculty of Engineering, Benha University, Cairo 11629, Egypt (e-mail: islam.mansour@feng.bu.edu.eg).

Mohamed Aboualalaa is with the Electronics Research Institute (ERI), Giza 12622, Egypt (e-mail: mohamed.ali@ejust.edu.eg).

Adel Barakat is with the Center for Japan-Egypt Cooperation in Science and Technology, Kyushu University, Fukuoka 819-0395, Japan.

Ahmed Allam is with the Department of Electronics and Communications Engineering (ECE), Egypt-Japan University of Science and Technology, Alexandria 21934, Egypt.

Adel B. Abdel-Rahman is with the Department of Electronics and Communications Engineering (ECE), Egypt-Japan University of Science and Technology, Alexandria 21934, Egypt, and also with the Electrical Engineering Department, Faculty of Engineering, South Valley University, Qena 83523, Egypt.

Mohammed Abo-Zahhad is with the Department of Electronics and Communications Engineering (ECE), Egypt-Japan University of Science and Technology, Alexandria 21934, Egypt, and also with the Electrical and Electronics Engineering Department, Faculty of Engineering, Assiut University, Assiut 71515, Egypt.

Ramesh K. Pokharel is with the Faculty of Information Science and Electrical Engineering, Kyushu University, Fukuoka 819-0395, Japan.

Color versions of one or more of the figures in this letter are available online at http://ieeexplore.ieee.org.

Digital Object Identifier 10.1109/LMWC.2020.3004753

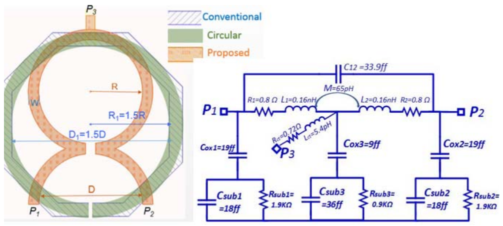

(a) (b)

Fig. 1. (a) Layout of the conventional CT inductor and the proposed CT inductor. (b) Equivalent circuit of the proposed CT inductor.

TABLE I

INDUCTANCE AND LOSS OF CONVENTIONAL, CIRCULAR, AND PROPOSED

Parameters	Conventional	Circular	Proposed	Unit
Width (W)	9	9	9	µm
Length (l)	280.6	282.6	282.6	µm
Area (A)	0.028	0.0254	0.0169	mm^2
Self-inductance (L_s)	252	256	256	pH
Mutual inductance (M)	>38.3	>39.2	>52.4	pH
Loss resistance (R_s)	2.82	2.8	2.8	Ω

proposed inductor that has the same length. The area of the conventional inductor and the proposed shape are calculated as

$$A_{\text{conventional}} \approx \pi * R_1^2 = \frac{9}{4}\pi * R^2 \quad (1)$$

$$A_{\text{proposed}} = \pi R^2 + 0.5 * \pi R^2 = \frac{3}{2}\pi * R^2. \quad (2)$$

To achieve a specific inductance, the proposed structure becomes compacted by a ratio of $A_{\text{proposed}}/A_{\text{conventional}} = 2/3$.

The inductance of one arm (L_s), mutual inductance between two arms (M) and loss resistance (R_s) of the inductor can be calculated using the following equations [14]:

$$L_s = \frac{\mu l}{2\pi}\left[\ln\left(\frac{2l}{W}\right) + 0.5 + \frac{W}{3l} - \frac{W^2}{24l^2}\right] \quad (3)$$

$$M = \frac{\mu l}{2\pi}\left[\ln(2l) - \ln(D) - 1 + \frac{D}{l} - \frac{D^2}{4l^2}\right] \quad (4)$$

$$R_s = \frac{l}{\sigma W \delta(1 - e^{-t/\delta})} \quad (5)$$

where l = length of one arm, W = width of the wire, D = gap between two arms, σ = conductivity of the metal, t = thickness of wire, and $\delta = 1/(\pi\mu_0\sigma f)^{1/2}$ = skin penetration depth.

M is the mutual inductance between the two inductors and mainly depends on the separation between two coils and the shape of the planar coils [15]. The total differential inductance will be enhanced by $2M$. The circular shape achieves the highest coupling, lowest resistance, and best quality factor. Table I summarizes the calculated parameters of the conventional circular and the proposed inductor at 13 GHz. As shown in Table I, the proposed structure has higher mutual inductance than the conventional one and occupies less area.

The equivalent circuit model for the proposed CT inductor is shown in Fig. 1(b).

The proposed CT inductor is designed and electromagnetically (EM) simulated using ANSYS high-frequency structure simulator (HFSS), and advanced design systems (ADS) Momentum. The differential inductance (L_{diff}), Q-factor (Q_{diff}), self-inductances (L_1 and L_2), coupling coefficient (K) where $0 < K < 1$, and the mutual inductance (M) between the two arms of CT inductor are calculated using the following

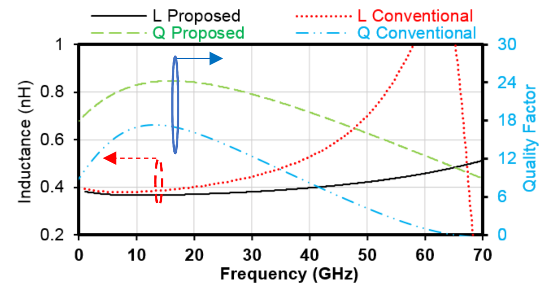

Fig. 2. Comparison of Q-factor and inductance of the proposed CT inductor and the conventional CT inductor.

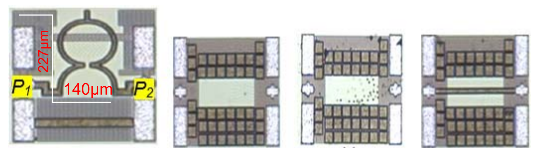

(a) (b) (c) (d)

Fig. 3. Die photo of (a) fabricated CT inductor, (b) open, (c) short, and (d) through structures.

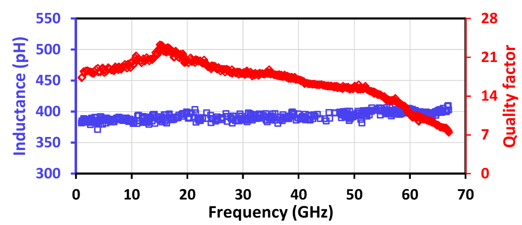

Fig. 4. Measured inductance and quality factor of the fabricated CT inductor.

equations:

$$Z_{\text{diff}} = 2(Y_{23} + Y_{13})/Y_{23}(Y_{11} - Y_{12}) - Y_{13}(Y_{21} - Y_{22}) \quad (6)$$

$$L_{\text{diff}} = \text{Im}(Z_{\text{diff}})/\omega \text{ and } Q_{\text{diff}} = \text{Im}(Z_{\text{diff}})/\text{Re}(Z_{\text{diff}}) \quad (7)$$

$$L_1 = L_2 = \text{Im}(Z_{11})/\omega = \text{Im}(Z_{22})/\omega \quad (8)$$

$$K = \text{Im}(Z_{21})/\sqrt{\text{Im}(Z_{11}) \times \text{Im}(Z_{22})}$$

$$\text{and } M = K \times \sqrt{L_1 \times L_2}. \quad (9)$$

The proposed CT inductor has a differential inductance that is close to 0.38 nH, mutual-inductance of 0.06 nH, while the coupling coefficient between two arms equals 0.37. A comparison between the Q-factor and the inductance of the conventional and the proposed CT inductors is shown in Fig. 2. The proposed CT inductor has an improved Q-factor that increased by 41% than that of the conventional one. Also, the self-resonance frequency of the proposed CT inductor is 115.7 GHz, which is much higher than that of the conventional one (69 GHz). The inductor area is compacted from 0.065 to 0.032 mm^2 due to the new structure.

III. EXPERIMENTAL RESULTS OF THE PROPOSED INDUCTOR

The proposed inductor was implemented in the 0.18-μm CMOS technology. Fig. 3(a) shows the fabricated inductor and the corresponding deembedding structures, open, short, and through, are shown in Fig. 3(b)–(d). These additional structures are required for the deembedding procedure. The deembedding method includes the subtraction of the parasitic shunt Y-parameters of the on-wafer open calibration pattern as well as the subtraction of the parasitic series Z-parameters on the on-wafer open circuit which are taken from measurements of the short and through circuits [16]. We performed the measurement using the Keysight vector network analyzer (VNA) E8361C, which allows characterization up to 67 GHz.

TABLE II

COMPARISON OF DIFFERENT SHAPED INDUCTOR DESIGNS

Parameter	[12]	[17]	[18]	Proposed
L_{diff} (pH)	615	500	900	385
Max Q_{diff}	14@12GHz	16@12 GHz	9@ 6GHz	22@12 GHz
Shape	8-shape	8-shape	Circular	Circular &half

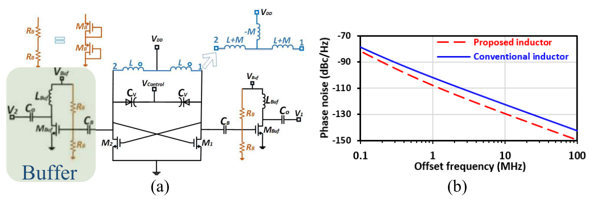

Fig. 5. (a) Schematic of the VCO and (b) phase noise improvement due to the proposed inductor.

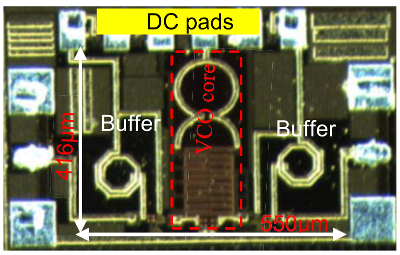

Fig. 6. Die photo of the fabricated VCO.

TABLE III

VCO PERFORMANCE USING CONVENTIONAL AND THE PROPOSED INDUCTOR

Parameters	Proposed	Conventional
Phase noise @1MHz	-108.7	-103
Output power	-4 dBm	-9 dBm
Inductor size	0.032 mm^2	0.065 mm^2

The measured inductance and Q-factor are shown in Fig. 4. The inductance is 385 pH in the *Ku*-band with a maximum Q-factor of 23.5 at 15 GHz as shown in Fig. 4.

Table II summarizes the performance of the fabricated inductor compared to other published inductor designs. The measured differential Q-factor reaches 22 at 12 GHz when the inductance is 385 pH. This achieved high-quality factor improves the performance of VCOs and is high enough for most broadband VCO designs.

IV. IMPLEMENTATION AND EXPERIMENTAL RESULTS OF VCO

The proposed high-Q inductor is used in the tank circuit of the VCO shown in Fig. 5(a), which improves the phase noise as shown in Fig. 5(b), compacted the VCO size, and increases the output power as illustrated in Table III.

Fig. 6 shows a photograph of the fabricated die where the VCO core is only 140 μm $\times$ 400 μm, and the total die area is 0.2288 mm^2 including the two output buffers.

An FSUP signal source analyzer was used in the measurement. The dc power consumption of the VCO is 4 mW from a supply voltage of 1 V in the whole frequency tuning range (FTR) which equals 16% from 11.7 to 13.7 GHz as shown in Fig. 7. The measured phase noise of the proposed VCO at 1 and 10-MHz offset frequencies is displayed in Fig. 7. The designed VCO shows a phase noise of -107.7 and 126.13 dBc/Hz at 1 and 10 MHz offset with the variation of 1.7 and 2 dBc/Hz, respectively, based on the frequency.

The measured and simulated phase noises are shown in Fig. 8 with a difference about ± 2 dB. The proposed VCO

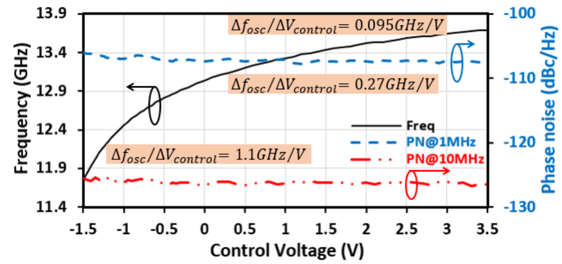

Fig. 7. Measured frequency tuning range and phase noise of the proposed VCO.

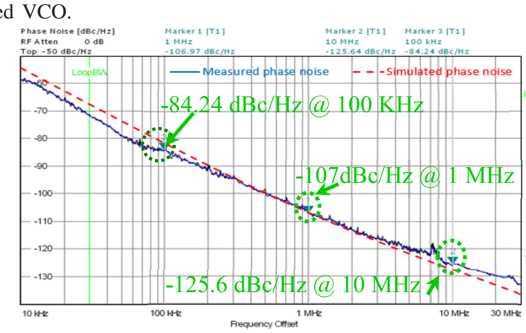

Fig. 8. Measured and simulated phase noise spectrum.

TABLE IV

PERFORMANCE COMPARISON OF *Ku*-BAND VCOS

Ref	Tec. CMOS	F_{osc} [GHz]	FTR [%]	P_{dc} mW	PN	Area [mm^2]	FoM	FoM^T	FoM$_A$
[2]	0.18μm	15	12	34	-100.2	0.08	-168.3	-170	-179.3
[5]*	0.18μm	15.7	5.8	5	-105	0.08	-182	-177.3	-192.7
[19]	0.13μm	14	13.3	0.6	-100.6	0.45#	-186	-188.3	N.A
[20]	65nm	10.6	9.6	2.2	-107.7	0.07	-185	-185	-196
[21]	0.25μm	12.8	5.1	93	-123	0.25	-183	-177.2	-189
[22]	90nm	12.8	1.64	3	-105.3	0.22#	-182.6	-166.9	N.A
[23]	0.18μm	14.6	7.12	3	-109.3	0.098	-187.8	-184.8	-199
This	**0.18μm**	**12.7**	**16**	**4**	**-107.7**	**0.056**	**-184.4**	**-188.5**	**-197**

$FoM = PN - 20\log\left(\frac{f_{osc}}{\Delta f}\right) + 10\log(P_{dc})$, $FoM^T = FoM - 20\log\left(\frac{FTR}{10}\right)$ and $FoM_A = FoM + 10\log(A)$ * FoM is re-calculated for 1MHz offset frequency, # total area including pads.

has a wide tuning range and very compact size compared to the other reported *Ku*-band VCOs, it achieves the highest FoM^T and FoM$_A$ as illustrated in Table IV.

V. CONCLUSION

A *Ku*-band VCO using the proposed CT inductor in 0.18-μm CMOS technology has been proposed. The fabricated CT inductor has better Q-factor, wideband characteristics, and compact size compared to conventional CT inductor. The measured inductance and quality factors are 385 pH and 22, respectively, at 12 GHz. As a result, the proposed VCO has a tuning range of 2 GHz from 11.7 to 13.7 GHz, a phase noise of -107.7 dBc/Hz at 1-MHz offset frequency while drawing 4-mW power. The FoM^T and FoM$_A$ are -188.6 and -197 dBc/Hz, respectively. Benefiting from the proposed inductor design technique, the proposed VCO accomplishes the best FoM^T and FoM$_A$ among the previously proposed state-of-the-art *LC*-VCOs.

REFERENCES

[1] A. Zolfaghari, A. Chan, and B. Razavi, "Stacked inductors and transformers in CMOS technology," *IEEE J. Solid-State Circuits*, vol. 36, no. 4, pp. 620–628, Apr. 2001.

[2] M. K. Chirala and C. Nguyen, "An extremely miniaturized 15-GHz CMOS distributed voltage-controlled oscillator," *Microw. Opt. Technol. Lett.*, vol. 51, no. 8, pp. 1953–1955, Aug. 2009.

[3] R. Murakami, T. Ito, K. Okada, and A. Matsuzawa, "An ultra-compact LC-VCO using a stacked-spiral inductor," *IEICE Electron. Express*, vol. 8, no. 7, pp. 512–517, 2011.

[4] R. Murakami, K. Okada, and A. Matsuzawa, "A 484-μm^2 21-GHz LC-VCO beneath a stacked-spiral inductor," in *Proc. IEEE 40th Eur. Microw. Conf. (EuMC)*, Paris, France, Sep. 2010, pp. 1615–1618.

[5] N. Jahan, S. A. E. Ab Rahim, A. Barakat, T. Kaho, and R. K. Pokharel, "Design and application of virtual inductance of square-shaped defected ground structure in 0.18-μm CMOS technology," *IEEE J. Electron Devices Soc.*, vol. 5, no. 5, pp. 299–305, Sep. 2017.

[6] N. Jahan, S. A. E. Ab Rahim, H. Mosalam, A. Barakat, T. Kaho, and R. K. Pokharel, "22-GHz-band oscillator using integrated H-shape defected ground structure resonator in 0.18-μm CMOS technology," *IEEE Microw. Wireless Compon. Lett.*, vol. 28, no. 3, pp. 233–235, Mar. 2018.

[7] I. Mansour, M. Aboualalaa, A. Allam, A. B. Abdel-Rahman, M. Abo-Zahhad, and R. K. Pokharel, "Dual band VCO based on a high-quality factor switched interdigital resonator for the Ku band using 180-nm CMOS Technology," *IEEE Trans. Circuits Syst II, Exp. Briefs*, vol. 65, no. 12, pp. 1874–1878, Dec. 2018.

[8] I. Mansour, H. Mosalam, A. Allam, A. B. Abdel-Rahman, and R. K. Pokharel, "K band low power voltage controlled oscillator using 180 nm CMOS technology with a new high quality inductor," in *Proc. IEEE Int. Conf. Ubiquitous Wireless Broadband (ICUWB)*, Oct. 2016, pp. 1–4.

[9] D. B. Leeson, "A simple model of feedback oscillator noise spectrum," *Proc. IEEE*, vol. 54, no. 2, pp. 329–330, Feb. 1966.

[10] J. M. Lopez-Villegas, J. Samitier, C. Cane, P. Losantos, and J. Bausells, "Improvement of the quality factor of RF integrated inductors by layout optimization," *IEEE Trans. Microw. Theory Techn.*, vol. 48, no. 1, pp. 76–83, Jan. 2000.

[11] C. P. Yue and S. S. Wong, "On-chip spiral inductors with patterned ground shields for Si-based RF ICs," *IEEE J. Solid-State Circuits*, vol. 33, no. 5, pp. 743–752, May 1998.

[12] W. Zou, D. Chen, W. Peng, and Y. Zeng, "Experimental investigation of multi-path and metal-stacking structure for 8-shape on-chip inductors on standard CMOS," *Electron. Lett.*, vol. 52, no. 24, pp. 1998–1999, Nov. 2016.

[13] V. N. Rao Vanukuru, "Enhanced q improvement in rectangular shaped inductors with tapered spirals," in *IEEE MTT-S Int. Microw. Symp. Dig.*, Nov. 2018, pp. 1–3.

[14] S. S. Mohan, "Modeling, design and optimization of on-chip inductors and transformers," Ph.D. dissertation, Dept. Center Integr. Syst., Stanford Univ., Stanford, CA, USA, Dec. 1999.

[15] S. Raju, R. Wu, M. Chan, and C. P. Yue, "Modeling of mutual coupling between planar inductors in wireless power applications," *IEEE Trans. Power Electron.*, vol. 29, no. 1, pp. 481–490, Jan. 2014.

[16] M. Drakaki, A. A. Hatzopoulos, and S. Siskos, "De-embedding method for on-wafer RF CMOS inductor measurements," *Microelectron. J.*, vol. 40, no. 6, pp. 958–965, Jun. 2009.

[17] W. Zou, X. Zou, D. Ren, K. Zhang, D. Liu, and Z. Ren, "2.49-4.91 GHz wideband VCO with optimised 8-shaped inductor," *Electron. Lett.*, vol. 55, no. 1, pp. 55–57, Jan. 2019.

[18] T. N. Nguyen and J.-W. Lee, "Ultralow-power Ku-band dual-feedback armstrong VCO with a wide tuning range," *IEEE Trans. Circuits Syst. II, Exp. Briefs*, vol. 59, no. 7, pp. 394–398, Jul. 2012.

[19] W. Y. Yin, S. J. Pan, L. W. Li, and Y. B. Gan, "Modelling on-chip circular double-spiral stacked inductors for RFICs," *IEE Proc. Microw. Antennas Propag.*, vol. 150, no. 6, pp. 463–469, Dec. 2003.

[20] M. T. Amin, J. Yin, P.-I. Mak, and R. P. Martins, "A 0.07 mm^2 2.2 mW 10 GHz current-reuse class-B/C hybrid VCO achieving 196-dBc/Hz FoM$_A$," *IEEE Microw. Wireless Compon. Lett.*, vol. 25, no. 7, pp. 457–459, Jul. 2015.

[21] Y. Wang, D. Leenaerts, E. van der Heijden, and R. Mahmoudi, "A low phase noise colpitts VCO for Ku-band applications," in *Proc. IEEE Bipolar/BiCMOS Circuits Technol. Meeting (BCTM)*, Portland, OR, USA, Sep. 2012, pp. 1–4.

[22] D. Zito, D. Pepe, and A. Fonte, "13 GHz CMOS active inductor LC VCO," *IEEE Microw. Wireless Compon. Lett.*, vol. 22, no. 3, pp. 138–140, Mar. 2012.

[23] Z.-Y. Yang and R. Y. Chen, "High-performance low-cost dual 15 GHz/30 GHz CMOS LC voltage-controlled oscillator," *IEEE Microw. Wireless Compon. Lett.*, vol. 26, no. 9, pp. 714–716, Sep. 2016.